

FLOW OF HYDROGEN FROM BURIED LEAKS

Atkinson, G.¹, Hooker, P.², Hall, J.³, and Hawksworth, S.J.⁴

¹ Science Division, Health and Safety Executive, Harpur Hill, Buxton, SK17 9JN, UK,
graham.atkinson@hse.gov.uk

² Science Division, Health and Safety Executive, Harpur Hill, Buxton, SK17 9JN, UK,
philip.hooker@hse.gov.uk

³ Science Division, Health and Safety Executive, Harpur Hill, Buxton, SK17 9JN, UK,
jonathan.hall@hse.gov.uk

⁴ Science Division, Health and Safety Executive, Harpur Hill, Buxton, SK17 9JN, UK,
stuart.hawksworth@hse.gov.uk

ABSTRACT

The substitution of hydrogen for natural gas within a gas network has implications for the potential rate of leakage from pipes and the distribution of gas flow driven by such leaks. This paper presents theoretical analyses of low-pressure flow through porous ground in a range of circumstances and practical experimental work at a realistic scale, using natural gas, hydrogen or nitrogen for selected cases. This study considers flow and distribution of 100% hydrogen.

A series of eight generic flow regimes have been analysed theoretically e.g. (i) a crack in uncovered ground (ii) a crack under a semi-permeable cover in a high porosity channel (along a service line or road). In all cases the analyses yield both the change in flow rate when hydrogen leaks and the change in distance to which hydrogen gas can travel at a dangerous rate compared to natural gas. In some scenarios, a change to hydrogen gas from natural gas makes minimal difference to the range (i.e. distance from the leak) at which significant gas flows will occur. However, in cases where the leak is covered by an impermeable membrane, a change to hydrogen from natural gas may extend the range of significant gas flow by tens or even hundreds of metres above that of natural gas.

Experimental work has been undertaken in specific cases to investigate the following: (i) Flow rate vs pressure curves for leaks into media with different permeability, (ii) Effects of the water content of the ground on gas flow, (iii) Distribution of surface gas flux near a buried leak, and (iv) Distribution of surface gas flux where gas escapes at the edge of an impermeable cover.

THEORETICAL STUDIES

FACTORS AFFECTING GAS FLOW

Movement of gas away from a buried leak are driven by source pressure, buoyancy and diffusion. It has been shown that buoyancy driven flows and diffusion significantly affect the movement of light gases (including hydrogen) from very small leaks [1,2], although the contamination of ground at a significant distance (several metres) from the source only occurred over a very long time period.

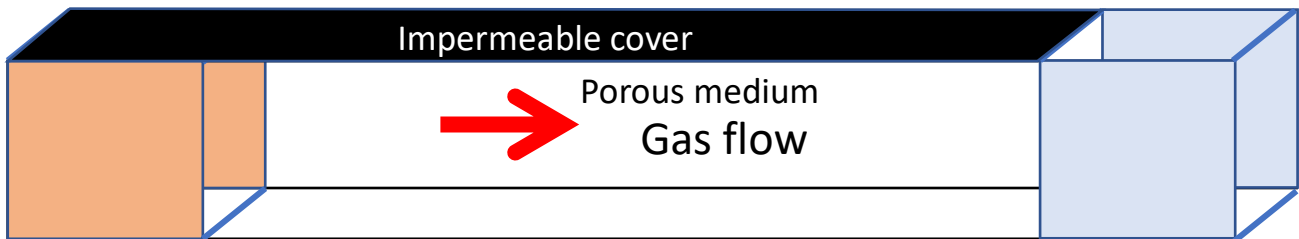
In practice the risk of gas accumulating to a dangerous (i.e. flammable) concentration within an enclosed space (referred to here as a “target”) is a function of the flux of gas into the space and the ventilation rate within the space. This is shown for typical real-world situations in Table 1. Where the flux of gas is very small, the risk of accumulation to dangerous concentrations is low in any space, with even a small level of ventilation

Table 1: Typical level of risk for various levels of sub-surface gas flux.

Gas flux (litres/s/m ²)	Level of risk	Vulnerable targets

<0.01	Usually negligible	-
> 0.01 and <0.1	Low risk	Small, poorly-ventilated spaces e.g. cupboards
> 0.1 and <1	Moderate	Rooms with low levels of ventilation
> 1 and <10	High	Rooms and small buildings
>10	Very High	Many buildings

It is important to determine whether buoyant or diffusive flows are important when considering the risk of dangerous gas accumulations occurring in practical gas distribution situations.



Source

Target

Figure 1: Schematic of Worst-case migration of gas under an impermeable cover into a vulnerable target (e.g. a cellar or permeable floor) through a relatively porous channel in compacted ground.

Figure 1 shows a porous channel, 1m in depth and 1m wide, with the medium having a permeability of $3 \times 10^{-11} \text{ m}^2$ (typical for pit sand). A series of typical flow rates, driven by medium and low-pressure sources, buoyancy and diffusion for hydrogen and natural gas, have been calculated for this situation, as shown in Figure 2.

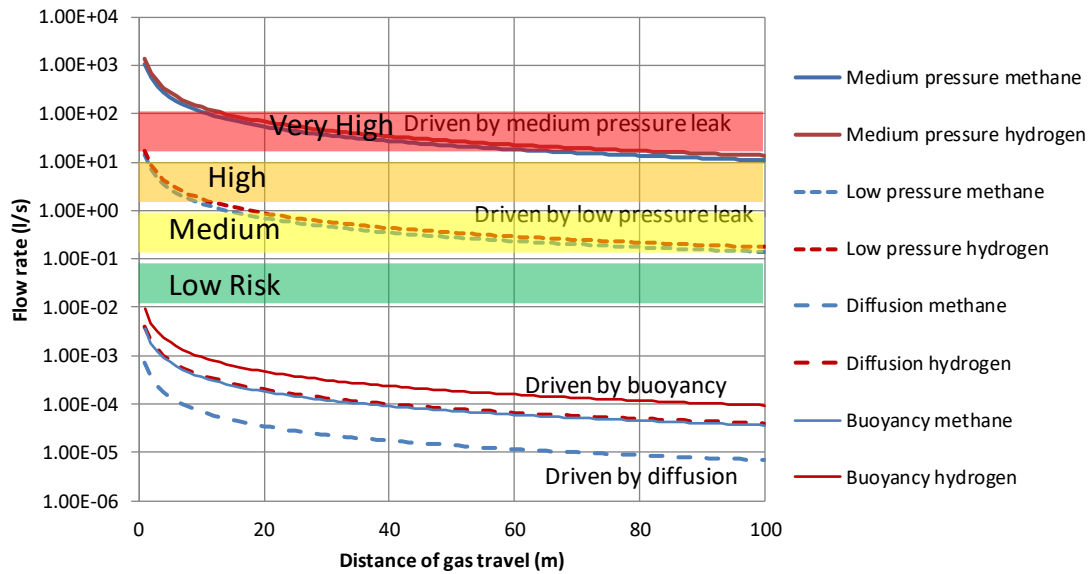


Figure 2: Flow rates driven by different mechanisms and risk level

The figure shows that relative effects of pressure and gas type on observed flow rate at distance from the source of the leak. For both low and medium pressures, there is little difference in the response between methane and hydrogen in the relationship between leak rate and distance of gas travel indicating that leak pressure is the driver for distance travelled. As leak pressure reduces so as to become negligible on the gas dispersion mode, divergence of each material type under similar conditions occurs as would be expected due to dominance of molecular volume and gas density on these properties. Figure 2 also suggests that although the low density and high diffusivity of hydrogen relative to natural gas do lead to a potential increase in flow rates when driven by buoyancy forces and diffusion, these increases are such low level to be normally negligible in determining the potential rate of change of gas accumulation in vulnerable spaces. Conversely, medium pressure leaks can present a Very High risk even if gas must flow a distance of order 100m through porous ground while low pressure leaks can present a High risk even where the gas release flows a distance of order 10m through porous ground.

FLOW ANALYSIS

Where release pressures are sufficiently high that buoyancy force and diffusion-controlled processes can be ignored, pressure driven flows can be predicted using Darcy’s Equation. Pressure P (a scalar field) and velocity \underline{u} (a vector) are related as:

$$-\nabla P = \frac{\mu}{\kappa} \underline{u} \quad \mu \text{ is the gas dynamic viscosity and } \kappa \text{ is the permeability of the ground} \quad [1]$$

Or, for high flow speeds, the generalised equation including inertial forces

$$-\nabla P = \frac{\mu}{\kappa} \underline{u} + F|\underline{u}|\underline{u} \quad F \text{ is a constant} \quad [2]$$

For low pressure leaks in typical ground Darcy’s Equation is a good representation of reality. Analysis shows that inertial corrections are required for higher pressure leaks and for very porous ground e.g. coarse gravel.

The equations for viscous flow from a source through porous ground mirror those for other phenomena, such as the potential and electric field induced by charges, and so standard solutions and methods of analysis can be applied.

Flow from a buried source in an infinite porous medium

For the purposes of analysis, the gas leaving the hole in the pipe can be considered to form a cavity in the ground at the site of the hole. Gas flows out of a cavity radius r_i (i=inner) at a rate Q (Figure 3). The pressure in the cavity is P_i .

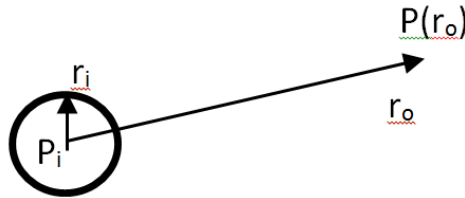


Figure 3: Schematic showing flow from a buried source

The pressure $P(r_o)$ at a radius r_o (o=outer) is given by

$$P_i - P(r_o) = \int_{r_i}^{r_o} \frac{\mu}{\kappa} \frac{Q}{4\pi r^2} dr = \frac{Q}{4\pi} \cdot \frac{\mu}{\kappa} \left[\frac{1}{r_i} - \frac{1}{r_o} \right] \quad [3]$$

Where the cavity is similar in size to the hole in a pipe, most of the pressure drop is close to the hole in a pipe. For a 10 mm diameter hole the pressure falls to 10% of line pressure within a distance of 100 mm.

The induced (vector) velocity is

$$\underline{u} = \frac{Q}{4\pi r^2} \hat{r} \quad [4]$$

1.2.2 Flow from a buried source close to a free surface

This can be solved using the method of images [3] – the flow mirrors the electric field of a dipole. Adding a negative image source in the symmetry position above the free surface ensures that the flow is perpendicular to the free surface (there can be no transverse flow since this would lead to transverse pressure gradients and discontinuities in pressure across the surface).

The velocity and pressure induced are (subscripts + refer to the source and – to the negative image)

$$\underline{u} = \frac{Q}{4\pi} \left(\frac{\hat{r}_+}{r_+^2} - \frac{\hat{r}_-}{r_-^2} \right) \quad \text{and} \quad P = \frac{Q}{4\pi} \cdot \frac{\mu}{\kappa} \left[\frac{1}{r_+} - \frac{1}{r_-} \right] \quad [5]$$

The volume flux through the surface from a leak buried to depth h at a distance r from the centre is

$$\text{Surface Flux} = \frac{Q}{2\pi} \cdot \frac{h}{(h^2 + r^2)^{3/2}} \quad [6]$$

The flux falls off rapidly with distance from the centre – falling to 10% of the maximum at $r/h = 1.9$ and 1% of the maximum value at $r/h = 4.5$.

1.2.3 Flow from a buried source below a free surface and above an impermeable lower layer (e.g. a water table)

Where a gas leak is encountered below a free surface but above an impermeable lower layer such as a water table, the flow problem can be solved by a summation over a series of image sources. If the source of a leak is at a depth **a** below the free surface but also at height **b** above the impermeable lower layer, then the surface flux (**F**) is given by a series of the form:

$$F = \frac{Q}{2\pi} \cdot \frac{a}{(a^2 + r^2)^{3/2}} + \frac{Q}{2\pi} \cdot \sum_{n=1}^{\infty} \frac{(-1)^{n-1} [2n(a+b) - a]}{\{[2n(a+b) - a]^2 + r^2\}^{3/2}} + \frac{Q}{2\pi} \cdot \sum_{n=1}^{\infty} \frac{(-1)^n [2n(a+b) + a]}{\{[2n(a+b) + a]^2 + r^2\}^{3/2}}$$

Accurate calculation of flux close to the source require about four terms in the series for convergence (i.e insignificant change if additional terms are added). For a point that is ten times further from the source than the burial depth about twenty terms are required.

Figure 4 shows how the maximum surface flux varies with the location of the impermeable lower layer. The figure shows that surface gas flux can be significantly increased by the presence of an impermeable layer below the leak but only where the impermeable lower layer is close below the leak. The presence of the impermeable layer becomes negligible at approximately three times the depth of the pipe, indicating that there is little or no interaction between the gas from the release and the impermeable layer.

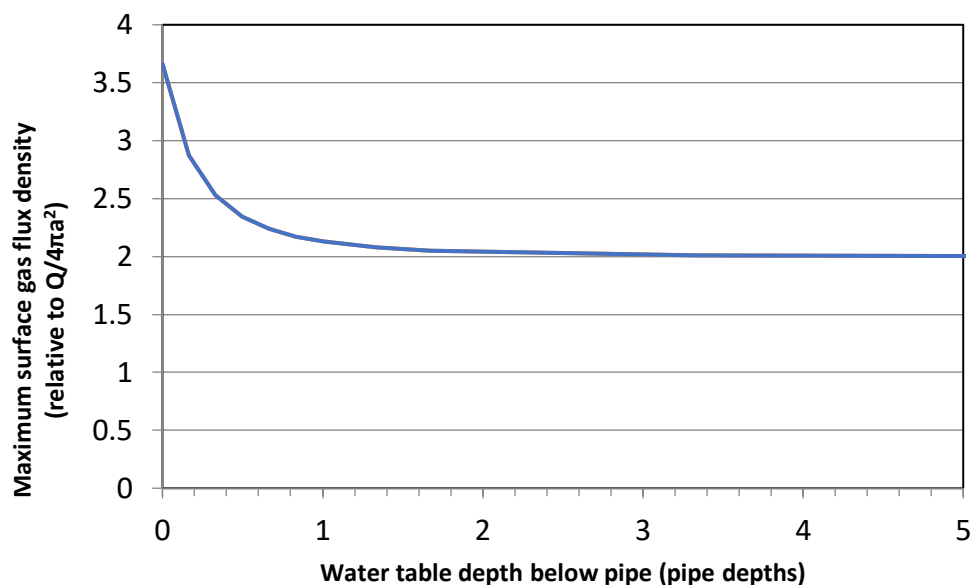


Figure 4: Maximum surface gas flux as a function of water table location below a leak.

COMPARISON OF RISK RANGES FOR HYDROGEN AND NATURAL GAS

Analyses based on Darcy's Equation have been used to compare the range to which a significant level of risk extends for hydrogen and natural gas supply. In different circumstances, risk could be related to levels of mass, energy or volume flow of feed gas. Lower Flammable Limit (LFL) concentrations for methane and hydrogen are similar (4.4% v/v cf. 4.0% v/v) and so to predict the risk of an explosion within a given space, within which there is an equal, fixed, level of ventilation and gas supply pressure, the risk is directly related to the volume flow of methane or hydrogen into the space.

Eight flow scenarios have been analysed. Two examples that represent readily feasible real world scenarios are shown in 1.3.1 and 1.3.2. A summary of all eight scenarios and results is given in Table 2.

Scenario 1- Flow from a buried source below a free surface – pressure drop across medium

For flow from a buried source below a free surface, and for a given hole geometry and supply pressure, the total flow from the leak for methane and hydrogen are in proportion to the reciprocal of viscosity:

$$\frac{Flow(hydrogen)}{Flow(methane)} = \frac{\mu(methane)}{\mu(hydrogen)} \approx 1.25$$

Solution of Darcy’s Equation (see 1.2) with appropriate boundary conditions gives:

$$Flux\ from\ surface \propto \frac{1}{L^3}$$

where L is distance between leak and target (assumed large relative to burial depth). Consequently, to offset an increase in surface flux by a factor of 1.25, an increase in distance L by a factor of $1.25^{1/3} \sim 1.08$ would be required. .

Scenario 5 – High porosity channel under a semi-permeable cover

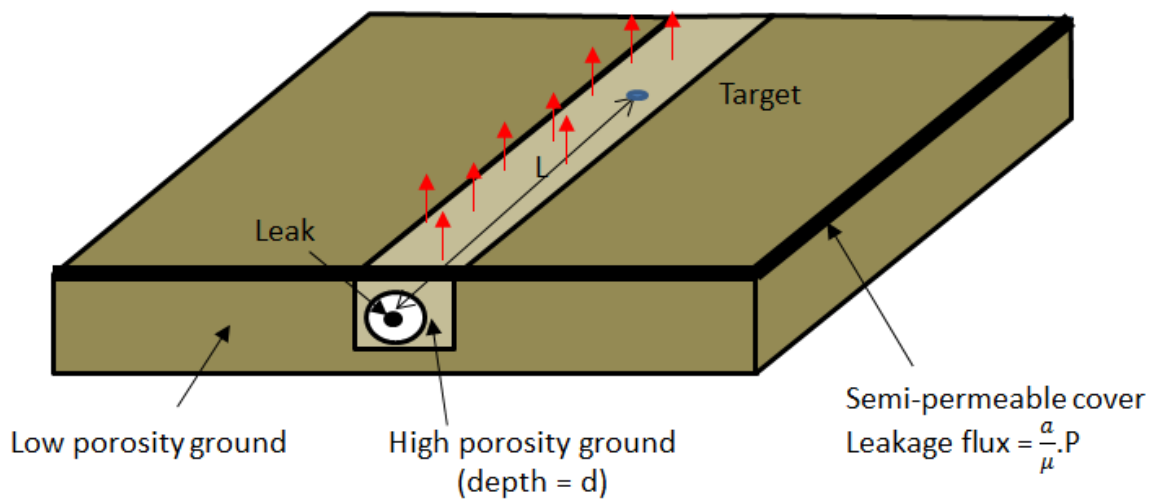


Figure 5: Schematic of underground leak in porous medium that is covered by a semi-permeable layer

In the scenario shown in Figure 5, a leak occurs underground, the gas flows through a porous medium that itself is covered by a semi-permeable layer. Therefore, some gas is released from the ground as the main flow proceeds underground. The target in the figure shows a low resistance path to a vulnerable space where gas accumulation could be dangerous.

The leakage through the semi-permeable cover is governed by the bulk permeability and thickness of the covering material, and described by the term, “a”. The bulk permeability of the porous medium under the cover is given the term “κ”.

Comparing hydrogen and methane flows at the leak point results in the following relationship:

$$\frac{Flow(hydrogen)}{Flow(methane)} = \left(\frac{\rho(methane)}{\rho(hydrogen)} \cdot \frac{P(hydrogen)}{P(methane)} \right)^{\frac{1}{2}}$$

Applying Darcy’s Law to the vented flow along the porous channel gives a relationship between the pressure within the ground and the distance from the leak point: $Pressure \propto e^{-\left(\frac{a}{\kappa d}\right)^{\frac{1}{2}}L}$

For equivalent flow rates of hydrogen and methane at the target point, it is necessary to offset the difference in density (by a factor of nine) requiring a nine-fold decrease in the pressure at the leak point.

This implies an increase in L by a factor of $\ln(9) \left(\frac{\kappa d}{a}\right)^{\frac{1}{2}} \approx 2.2 \left(\frac{\kappa d}{a}\right)^{\frac{1}{2}}$. Substituting typical values for a, κ and d reveals that an increase in distance of the order of tens of metres could be expected.

OVERVIEW

In many cases the switch to hydrogen from natural gas makes minimal difference to the range at which significant gas flows will occur. If the ground around the leak is uncovered, the hydrogen or natural gas will typically escape within a few metres of the release point. In cases where the leak occurs in ground that is covered with an impermeable or semi-permeable surface, the switch to hydrogen may extend the range of significant gas flows by tens or even hundreds of metres.

In some cases the magnitude of the change in range depends on the criterion used for what level of gas flow constitutes a significant risk. If low gas fluxes are still considered to constitute a significant risk then the change in range may be large.

Table 2: Summary of all eight scenarios and results analysed

	Scenario	Important parameters	Increase in range when hydrogen substituted for methane	Typical values for increase in range
1	Open ground with flow limited solely by ground permeability	Viscosity ratio	+ 8% of range for methane	A few metres or less
2	Open ground with flow from small crack in pipe	Density ratio*	+ 44% of range for methane	A few metres
3	Impermeable cover with high porosity channel and main flow vented at target	Viscosity ratio*	+ 25% of range for methane	Tens of metres
4	Impermeable cover with high porosity channel and main flow vented a distance D from source	Density ratio*, Distance D Criterion for significant risk (gas flux)	Typically of order D	Extent of impermeable cover. Tens or potentially hundreds of metres.
5	Semi-permeable cover with high porosity channel	Channel porosity κ , Channel depth d Cover permeability a, Density ratio*	$2.2 \left(\frac{\kappa d}{a}\right)^{\frac{1}{2}}$	Tens of metres

6	Impermeable cover with high porosity surface layer and main flow to target	Viscosity ratio*, source and target conditions, gas flux criterion.	Change in viscosity has to be balanced by the factor $\ln(L/d)$	Tens or potentially hundreds of metres.
7	Impermeable cover with high porosity surface layer and main flow vented a distance D from source	Density ratio*, Distance D Criterion for significant risk (gas flux)	Typically of order D	Extent of impermeable cover
8	Semi-permeable cover with high porosity surface layer	As Scenario 5	$2.2 \left(\frac{\kappa d}{a} \right)^{\frac{1}{2}}$	Tens of metres

LOW RESISTANCE PATHS TO VULNERABLE TARGETS

The most serious potential consequences of gas leakage are associated with (rare) releases into large open channels that lead directly into vulnerable buildings. An example of this problem is a service duct that is not properly sealed where it enters a property. Some ducts (especially for gas pipes) are perforated in order that any leaked gas entering the duct can escape through perforations and percolate up through the ground to safety rather than reach a vulnerable target via a damaged seal.

Where turbulent flow is encountered through a crack to a vulnerable target and a simultaneous larger viscous flow to safety (e.g. flow out of an extended perforated duct through the ground), the volume flow to danger may increase by a factor of up to about 4.5 if hydrogen is substituted for natural gas. This is a significantly larger increase more than for simple turbulent flow through holes where the increase in flow rate caused by the lower density of hydrogen is around 2.9.

EXPERIMENTAL WORK

Experiments were carried out to test out some of the aspects of the theoretical analysis. The basic experimental rig used for this work was a pit-sand-filled steel tank 8 metres long, 1.5 metres wide and 1 metre high. Test gases hydrogen, natural gas¹ or nitrogen were injected into the rig from standard bottled supplies at a rate measured at the inlet. The rig was covered with a plastic tent so that the moisture content of the sand could be controlled. Over a period of several weeks (prior to the tests that involved adding water) the sand dried to a depth of 50-100 mm below the surface. Below this level the moisture content remained constant at approximately 3.4% w/w² and provided a set condition for the experiment. The porosity of the sand was 36 %³.

Two different experimental arrangements were investigated:

FLOW FROM AN EXTENDED LINEAR CAVITY

Gas was vented into a large buried cavity which was formed by a 7.5 m long inverted rectangular channel – 100 mm wide and 50 mm deep. Gas could escape from the whole of the lower surface of the channel into the sand. This corresponded to a leak into a cavity formed by shrinkage of ground away from the lower surface of a pipe or the leakage of gas from a perforated duct. An outlet of variable size

¹ Hydrocarbon content: Methane 93.48%, Ethane 4.79%, Propane 1.22%, Butanes 0.43%, Pentanes 0.08%. The natural gas use also contained small quantities of nitrogen and carbon dioxide - molecular weight 17.3 g/mol.

² Determined by drying to constant weight

³ Determined from the volume of water required to saturate a core sample.

to allow gas to escape without passing through the sand was included, corresponding to a turbulent leak into a vulnerable target, and the flow through this path measured. The relative flows through the sand and the turbulent leak path could be determined.

POINT SOURCE GAS RELEASE

Test gases were allowed to vent from a point source (i.e. a hole in a pipe) and the flux of gas at the surface was determined at a range of distances from the source. Gases were released from the open end of a vertical 2" pipe at a depth of 600 mm. Surface gas fluxes were measured by collecting gas below a set of very lightweight plastic diaphragms mounted on 100 mm diameter tubes set 50 mm into the sand (Figure 5). The weight of the plastic film exerted a backpressure of about 0.2 Pa on the collected gas, which is not expected to significantly affect the gas flux. The relative magnitude of gas flux at different locations could be inferred from the reciprocal of the time for the diaphragm to inflate to a particular extent. This was carried out under two conditions; with an unobstructed surface, and with the surface covered by an impermeable layer (Figure 6).

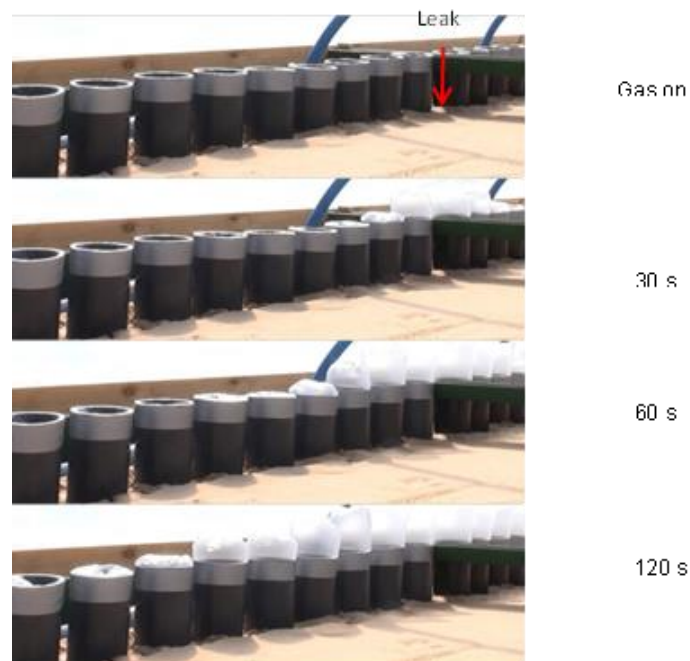


Figure 5: Lightweight plastic diaphragms used to monitor integrated surface volume flux

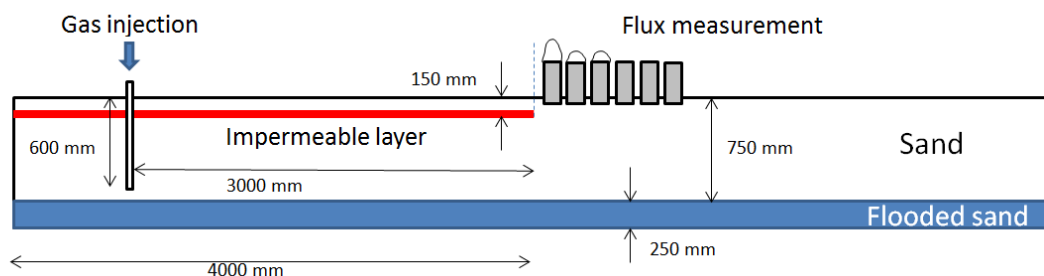


Figure 6: Schematic of experimental set up used to study flow at the edge of an impermeable cover

EXPERIMENTAL RESULTS

FLOW FROM AN EXTENDED LINEAR CAVITY

If the moisture content of the ground remains constant the flow closely follows Darcy's Equation (Figure 7).

Adding 480 litres of water (equivalent to 40 mm of rain) decreased permeability of the sand and this is shown in Figure 8. The apparent slight increases in hydrogen flow after wetting are traceable to changes in permeability as some excess water drained away over the time period needed to obtain pressure-flow data.

Larger decreases in permeability of sand (by a factor of about six) were observed in other tests following rapid, surface application of water equivalent to 75 mm of rain. However, these changes were short-lived and permeability returned to the original value within an hour, as excess water drained away. These tests were only carried out on pit-sand, but it seems likely that a given soil will often have the same permeability - at least in wet climates. The permeability might decrease after heavy rain, but will normally return to the original value, if excess water can drain away. Very prolonged drought would be required to dry out ground to the burial depth.

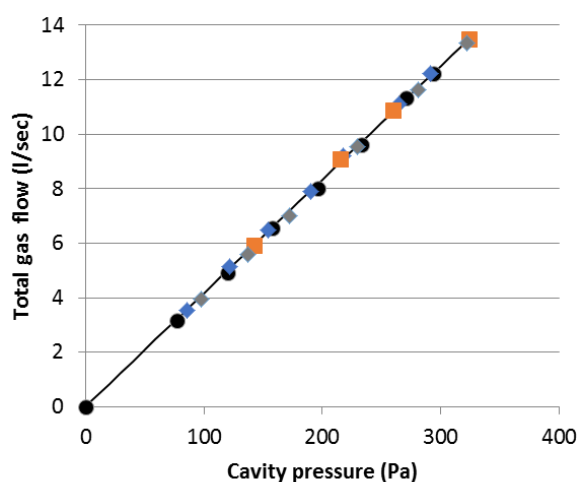


Figure 7: Repeated determinations of the pressure-flow characteristics at moderate flow rates

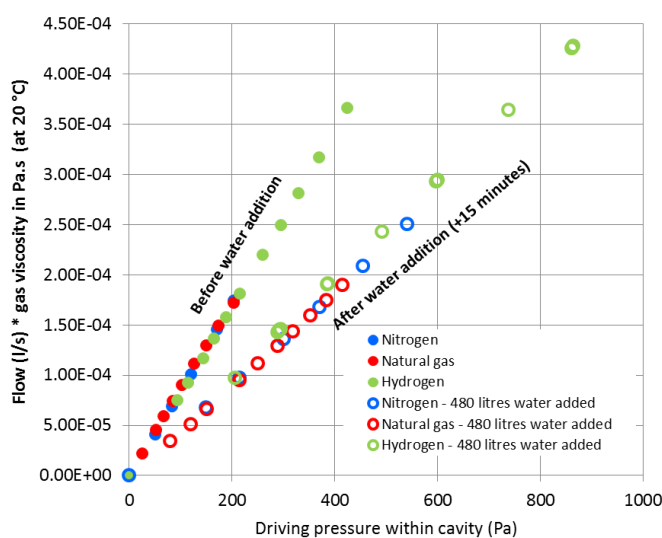


Figure 8: Effects of adding water on ground permeability (hydrogen tested last)

Tests were also carried out in which the gas could escape both (i) through the sand via the open boundary of the linear cavity and (ii) at a smaller rate through a small crack by-passing the sand. The results supported the analysis that predicts that in such circumstances the volume flow of hydrogen to a vulnerable target may exceed that for natural gas by a factor of up to about 4.5.

POINT SOURCE GAS RELEASE

The gas flux measurements, normalised to the average flux from the 5th and 6th sensors, are presented for all gases in Figure 9. Solutions of Darcy’s Equation for a point source and zero flux conditions at the tank walls were obtained for comparison and also shown in Figure 9.

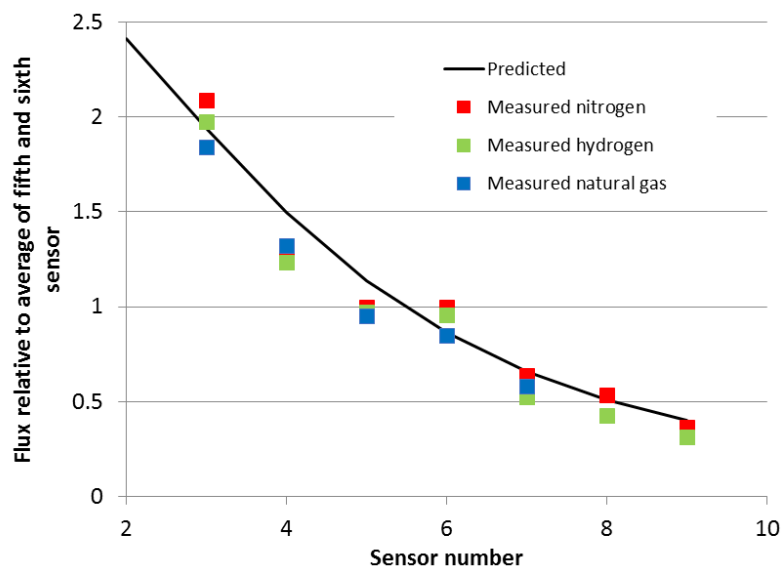


Figure 9: Comparison between predictions and measured flux for different gases

The distribution of flux (relative to the total flow) is very similar for all gases. The observed decay with distance also roughly matches that to be expected for a homogeneous porous medium. In fact, all the gases show similar deviations from the predictions which are presumably traceable to deviations from homogeneity e.g. varying levels of sand compaction. It is worth noting the total flows for similar inlets pressures and hole size did vary – as the reciprocal of viscosity.

Where an area immediately above a leak has an impermeable cover, gas will flow to the edge of the cover before escaping. It is generally not possible to simply write down solutions to Darcy’s Equation that satisfy these boundary conditions, but it is reasonable to assume that the gas will escape close to the edge i.e. on the length scale that is similar to the pipe depth D , rather than the horizontal distance from the leak point. Flux measurements were made at the edge of the impermeable cover (as illustrated in Figure 10).



Figure 10: Typical observation of flux at surface beyond the edge of an impermeable cover

Results confirmed that relatively small breaches in the cover will be very effective in completely preventing further progress of the gas. The effect of prolonged gas flow (at a high rate) in drying the medium and hence increasing permeability promoting flow was also observed.

CONCLUSIONS

A series of eight generic flow regimes were theoretically analysed corresponding to various flows under open and covered surfaces. In each the focus was on the distance to which gas can travel at a dangerous rate and how this distance varies if hydrogen is substituted for methane. This type of information allows more reliable application of safety data, accumulated during the operation of natural gas networks, to risk assessment for hydrogen supply.

In many cases the switch to hydrogen makes minimal difference to the range at which significant gas flows will occur. If the ground around the leak is uncovered, the hydrogen or natural gas will escape within a few meters of the release point. In cases where the leak is covered, the switch to hydrogen may extend the range of significant gas flows by tens or even hundreds of meters. The magnitude of the change in range may depend on the criterion used for what level of gas flow constitutes a significant risk.

The most serious potential consequences (largest flow rates) are associated with (rare) releases into large open channels that lead directly into vulnerable buildings. A clear example of this problem is a service duct that is not properly sealed where it enters a property.

Some key findings from the experimental programme were:

1. The measured flow rates of natural gas and hydrogen through sand at a range of conditions representative of gas distribution networks closely follow Darcy's Equation – measured flow rate was strictly proportional to pressure and the reciprocal of viscosity. There was no indication that inertial corrections at higher flow rates should be included in modelling.
2. Heavy surface application of water resulted in large decreases in gas permeability. These decreases were short lived dependent on dispersion of the water: permeability rapidly returned to close to the original value when water was allowed to drain.
3. Measurements of surface gas flux for various gases leaking from a point source under an open surface compared well with solutions of Darcy's Equation with appropriate boundary conditions. No differences traceable to differences in buoyancy and diffusivity were observed.

DISCLAIMER AND ACKNOWLEDGEMENTS

This report and the work it describes was undertaken by HSE's Research and Science Centre under contract to ERM. Its contents, including opinions and/ or conclusions expressed, or recommendations made, do not necessarily reflect the policy views of the Health and Safety Executive.

Funding of this work by the SGN H100 Project is gratefully acknowledged.

REFERENCES

[1] Okamoto, H. and Gomi, Y. (2011), "Empirical research on diffusion behaviour of leaked gas in the ground", Journal of Loss Prevention in the Process Industries, Vol 24, pp.531-540.

[2] Okamoto, H., Gomi, Y. and Akagi, H. (2014), "Movement characteristics of hydrogen gas within the ground and its detection at ground surface", Journal of Civil Engineering and Science, Vol 3, pp.49-66

[3] https://en.wikipedia.org/wiki/Method_of_images Last accessed 08/02/2019